Aggregate Preamble Sequence Design for Massive Machine-Type Communications in 5G Networks

Ahmed Elhamy Mostafa*, Vincent W.S. Wong*, Shuri Liao†, Robert Schober‡, Mengying Ding†, and Fan Wang†
* The University of British Columbia, Vancouver, Canada
† Huawei Technologies, Co. Ltd., Shanghai, China, ‡ Friedrich-Alexander-University, Erlangen, Germany
e-mail: {ahmedem, vincentw}@ece.ubc.ca, {liaoshuri, dingmengying, fan.wang}@huawei.com, robert.schober@fau.de

***Abstract*—Massive machine-type communications (mMTC) is a major use case in the fifth generation (5G) wireless networks. mMTC aims at supporting a large number of Internet of Things (IoT) connections within a coverage area. The current random access procedure in the Long Term Evolution (LTE) networks may not be able to handle a large number of simultaneous connection requests due to the limited number of random access preambles. Hence, it is essential to modify the random access procedure to support mMTC. In this paper, we propose a new preamble sequence design in which two Zadoff-Chu preamble sequences are aggregated together. This design enables us to have a larger set of random access preambles consisting of all combinations of pairing two Zadoff-Chu preamble sequences. Moreover, we consider a subset of all combinations that satisfy a certain maximum peak-to-average-power-ratio (PAPR) threshold criterion to reduce the energy consumption of the IoT devices. The proposed design requires only minor changes in the conventional transmitter and receiver design for generating and decoding the aggregated preamble sequences, respectively. Results show that the proposed design reduces the probability of preamble collision to less than 10^{-4}, which is lower than LTE. Furthermore, it outperforms other collision avoidance techniques such as access class barring (ACB) in terms of a lower average total service time. The modified receiver detects the aggregated preambles successfully and avoids detecting false preambles. Both the probabilities of misdetection and false alarm are less than 10^{-3} when the signal-to-noise ratio (SNR) is larger than -7 dB.**

I. Introduction

Machine-type communications (MTC) is a technology that enables a large number of devices to communicate with their servers with minimal human intervention. MTC is the main enabler of the Internet of Things (IoT) in the fifth generation (5G) cellular technologies, such as Long Term Evolution – Advanced (LTE-A) and New Radio. The number of connected IoT devices is expected to reach 3.3 billion by 2021 [1].

Massive machine-type communications (mMTC) is a major use case that will be supported by 5G cellular technologies [2]. mMTC aims to support a massive number of low-cost low-power IoT devices to send small payloads of delay-tolerant data. This use case includes applications such as smart homes, smart cities, wearables, and environmental sensing. The main requirements of mMTC are high connection density and low energy consumption. The number of simultaneous connections can be up to 1,000,000 connections per km^2 [3]. In addition, it is necessary to reduce the energy consumption and increase the battery lifetime of IoT devices to $10 - 15$ years.

Enhancing the random access procedure of 5G networks is a major challenge towards supporting mMTC [4]. The random access procedure is performed by a device to establish a connection with the base station before sending data packets. In this procedure, an IoT device sends a randomly selected preamble sequence. In LTE-A, there are 64 orthogonal preambles generated from Zadoff-Chu sequences as specified in [5]. However, preamble collision can happen if multiple devices select the same preamble within a single random access opportunity. With a massive number of concurrent random access requests, there is a high probability of preamble collision due to the limited number of preambles. Collisions cause devices to backoff and retransmit preambles. Subsequently, devices have to wait for a longer time to begin data transmission if multiple retransmissions are required. Battery-powered IoT devices also consume more energy due to these retransmissions. Hence, it is desirable to modify the random access procedure so that 5G networks can meet the requirements of mMTC.

To tackle the random access contention problem, multiple solutions have been proposed. Access class barring (ACB) reduces the random access contention by giving higher access probability to high priority devices [6]. ACB requires devices to have different priorities which may not be the case in mMTC. In [7], a group of IoT devices are clustered based on their locations and a single preamble is transmitted per cluster. Clustering reduces preamble transmissions but it entails the complexities of cluster formation and cluster head selection. In [8], non-orthogonal random access (NORA) is proposed to detect colliding preambles based on the differences in time of arrival. In [9], grant-free transmission allows devices to transmit their data directly which eliminates the random access process. The potential limitation of NORA and grant-free transmission is that they require complicated receivers to decode the superimposed preambles and data from multiple IoT devices, respectively.

The New Radio standard groups have proposed to perform multiple transmissions of either the same preamble or different preambles [10]. However, this option may result in a high physical random access channel (PRACH) overhead. Another option is to modify the preamble sequence design so that a larger set of preambles is available [11]. Preambles generated from Zadoff-Chu sequences are cyclic shifted versions of a basic sequence referred to as the root sequence. Reducing the cyclic shift value to generate more preambles may cause ambiguities at the receiver in case of large differences in the distances between the devices and the base station. Hence, a smaller cyclic shift requires a smaller coverage area for the base station, which makes it an inefficient solution.

In this paper, we propose to aggregate two preamble Zadoff-Chu sequences to generate up to $\binom{64}{2} = 2{,}016$ instead of 64 preambles for every Zadoff-Chu root sequence. The proposed design can reduce the average probability of preamble collision which enables 5G technologies (e.g. LTE-A and New Radio) to support mMTC use case. The new preamble sequences are generated and decoded by applying minor changes to the conventional LTE PRACH transmitter and receiver designs, respectively. We also propose to select a subset of the aggregated preambles with lower peak-to-average-power-ratio (PAPR) to reduce the energy consumption of the IoT devices. The main contributions of this paper are as follows:

- We propose a new preamble sequence design for mMTC based on aggregating two different Zadoff-Chu sequence preambles to increase the number of available random access preambles.
- We reduce the energy consumption of the IoT devices by selecting a subset of the aggregated preambles that satisfy a PAPR threshold constraint.
- Simulation results show that the proposed design reduces the probability of preamble collision to be less than 10^{-4}, which is lower than the conventional LTE PRACH. The proposed design also reduces the average total service time compared to ACB.
- Simulation results also show that the modified receiver can detect the aggregated preambles and avoid detecting false preambles. Both the probabilities of misdetection and false alarm are less than 10^{-3} when the signal-to-noise ratio (SNR) is larger than -7 dB.

The remainder of this paper is organized as follows. We present an overview of the random access procedure in Section II. The new preamble sequence design and its transmitter and receiver structures are presented in Section III. We evaluate the PAPR, the probability of preamble collision, the total service time, and the probability of preamble detection at the receiver in Section IV. Finally, Section V concludes the paper.

II. Random Access Procedure in LTE-A

In LTE-A, an IoT device establishes a connection with the base station before sending data by using a four-way handshake contention-based random access procedure as shown in Fig. 1 [12]. The IoT device first sends a randomly selected preamble during a random access opportunity (Step 1) and waits for a random access response (RAR) message from the base station (Step 2). Then, it sends a radio resource connection (RRC) request based on the information received in the RAR message (Step 3). Finally, the device waits for uplink radio resources grant for data transmission from the base station (Step 4). There are 64 orthogonal preambles generated from the Zadoff-Chu sequences as specified in [5]. Due to orthogonality, multiple preambles can be decoded by the base station at the same time. A collision between preambles can

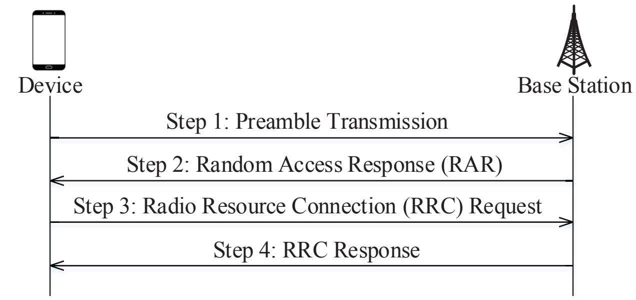

Fig. 1. Contention-based random access procedure in LTE-A systems [12].

happen if multiple IoT devices select the same preamble simultaneously, which is very probable in mMTC scenarios.

In LTE-A, orthogonal preamble sequences of length N_{zc} are generated using Zadoff-Chu sequences for a given root index l, where $l \in \mathcal{L} = \{1, \ldots, N_{zc}-1\}$, and cyclic shift N_{cs} [5]. Each preamble has a unique index m, where $m \in \mathcal{M} = \{1, \ldots, M\}$. We denote the preamble with index m that is generated using root index $l \in \mathcal{L}$ as s_m^l. The first preamble s_1^l is called the root sequence. The other preambles are generated by cyclically shifting the root sequence by multiples of N_{cs}. The number of orthogonal preambles per root M is given as

$$M = \lfloor N_{zc}/N_{cs} \rfloor, \tag{1}$$

where $\lfloor \cdot \rfloor$ denotes the floor function. When N_{zc} is equal to 839, which is used for LTE preamble formats $0-3$ [5], and N_{cs} is equal to 13, there are 64 preambles per root. Preambles can take different formats that differ in the length of the preamble sequence and the cyclic prefix. For channels with deep fading, longer sequence lengths and cyclic prefixes (e.g., format 3) are used to enhance reliability and combat fading.

III. New Preamble Sequence Design

In this section, we first present a new preamble sequence design. We then present the transmitter and receiver structures that generate and decode the proposed preamble sequences, respectively.

A. Preamble Aggregation

We propose to enlarge the set of preambles by adding two preamble sequences s_a^l, s_b^l having the same length, N_{zc}, where a, $b \in \mathcal{M}$ and $a \neq b$, for a given root index $l \in \mathcal{L}$. The resulting preamble pair sequence $q_{a,b}^l$ is given by

$$q_{a,b}^l[n] = \alpha_a s_a^l[n] + \alpha_b s_b^l[n], \quad \forall\, l \in \mathcal{L},\ a, b \in \mathcal{M},\ a \neq b, \\ 0 \leq n < N_{zc}, \tag{2}$$

where n is the discrete time index, α_a and α_b denote the power scaling coefficients of preambles s_a^l and s_b^l, respectively, such that $\alpha_a^2 + \alpha_b^2 = 1$. Hence, the number of preambles generated using one root index can be increased from $M = 64$ to $\binom{M}{2} = \binom{64}{2} = 2{,}016$. This reduces the probability of preamble collision in the random access procedure significantly. In addition, aggregating Zadoff-Chu sequences facilitates the implementation of the transmitter and receiver as only minimal upgrade is required when compared to the conventional transmitter and receiver in LTE-A. This facilitates the adoption of the proposed design in future standards. In fact, the transmitter only needs to average two preamble sequences and the receiver only needs to handle the detection of two preamble sequences to decode the aggregated preamble.

B. Transmitter Design

The transmitted signal x is generated as follows. First, two preamble sequences s_a^l and s_b^l are randomly selected and aggregated with power scaling coefficients α_a and α_b, respectively, to obtain $q_{a,b}^l$ as in (2). Then, the preamble pair $q_{a,b}^l$ is subject to the conventional processing of an LTE PRACH transmitter as shown in Fig. 2. The required changes with respect to the conventional PRACH transmitter are contained in the blue dashed box. Next, a discrete Fourier transform (DFT) of size N_{zc} is applied to $q_{a,b}^l$ to obtain the frequency domain representation $Q_{a,b}^l$, which is given by

$$Q_{a,b}^l[k] = \sum_{n=0}^{N_{zc}-1} q_{a,b}^l[n] \exp\left(\frac{-j2\pi nk}{N_{zc}}\right), 0 \le k < N_{zc}, \quad (3)$$

where k is the discrete frequency index. Then, we obtain the transmitted signal in the frequency domain, denoted as X in Fig. 2, after subcarrier mapping. This step is followed by an inverse discrete Fourier transform (IDFT) of size $(1/\Delta f_{\text{RA}} T_s)$, where Δf_{RA} is the preamble subcarrier spacing and T_s is the LTE basic time unit. In LTE-A, $\Delta f_{\text{RA}} = 1.25$ kHz and $1/T_s = 30.72$ MHz for preamble formats $0-3$, which results in an IDFT size of 24,576 [5]. After adding the cyclic prefix, the time domain transmitted signal $x[t]$ is given by

$$x[t] = \beta_{\text{PRACH}} \sum\nolimits_{k=0}^{N_{zc}-1} Q_{a,b}^l[k] \times \exp\left(-j2\pi(k+\varphi+K(k_0+0.5))\Delta f_{\text{RA}}(t-T_{\text{CP}})\right), \quad 0 \le t < T_{\text{CP}} + T_{\text{SEQ}}, \quad (4)$$

where β_{PRACH} is the PRACH amplitude scaling factor [5]. T_{CP} and T_{SEQ} are the cyclic prefix length and sequence length, respectively. φ, K, and k_0 are constant PRACH parameters that are used to map the transmitted signal to the proper subcarriers based on the preamble format as specified in [5]. The received signal $y[t]$ at the base station, assuming a frequency-selective fading channel having impulse response $h[j]$ with $J+1$ taps, is given by

$$y[t] = \sum\nolimits_{j=0}^{J} h[j]x[t-j] + z[t], \quad 0 \le t < T_{\text{CP}} + T_{\text{SEQ}}, \quad (5)$$

where $z[t]$ is complex additive white Gaussian noise (AWGN).

C. Receiver Design

Given the received signal y at the base station, the estimates of the transmitted preamble pairs of different devices can be obtained by directly correlating the received signal with all the preamble pairs $q_{a,b}^l$, $a, b \in \mathcal{M}$. However, this requires calculating the correlation with all 2,016 possible preamble pairs. This entails a high complexity and requires many changes to the conventional PRACH receiver.

Hence, we propose an alternative receiver design as shown in Fig. 3, which requires only one additional stage compared to the conventional PRACH receiver. This additional stage is referred to as the preamble pair detection stage, which is contained in the blue dashed box in Fig. 3. In particular, the received signal y is subject to cyclic prefix removal, DFT, and subcarrier demapping. The frequency domain representation of the received signal, denoted as $Y[k]$, is correlated with the conjugate of the frequency domain representation of the root sequence, denoted as S_1^l, of a given root index $l \in \mathcal{L}$. The resulting time correlation $c[n]$ can be expressed as

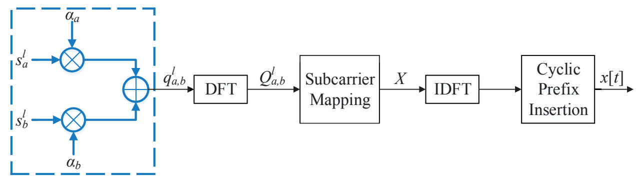

Fig. 2. Transmitter: Preambles s_a^l and s_b^l are scaled by α_a and α_b, respectively, and aggregated together. The resulting preamble sequence $q_{a,b}^i$ is subject to DFT, subcarrier mapping, IDFT, and cyclic prefix insertion.

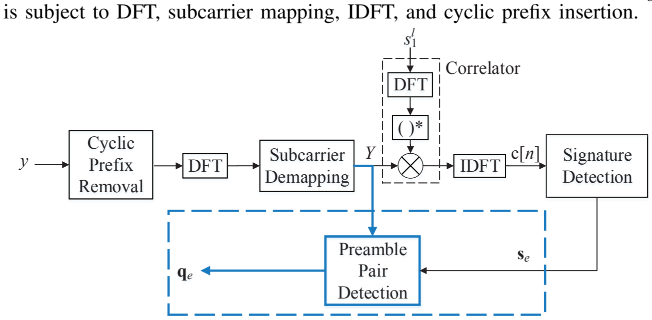

Fig. 3. Receiver: The received signal y is correlated with root sequence s_1^l to obtain time correlation $c[n]$ that is used to estimate the transmitted preambles, i.e., set $\mathbf{s}_e$. The preamble pair detection calculates the correlation between the received signal in the frequency domain and the subset of preamble pairs that can be generated using the preambles in set $\mathbf{s}_e$ to estimate the transmitted preamble pairs in set $\mathbf{q}_e$.

$$c[n] = \frac{1}{N_{\text{IDFT}}} \sum\nolimits_{k=0}^{N_{\text{IDFT}}-1} Y[k](S_1^l[k])^* \exp\left(\frac{j2\pi kn}{N_{\text{IDFT}}}\right), \quad 0 \le n < N_{\text{IDFT}}, \quad (6)$$

where N_{IDFT} is IDFT size, and $(\cdot)^*$ denotes complex conjugation. Since the other preamble sequences $s_2^l, \ldots, s_M^l$ are cyclically shifted versions of s_1^l, $c[n]$ represents the correlation with all preambles s_m^l, $m \in \mathcal{M}$. The range of n, $[0, N_{\text{IDFT}})$, is divided into M partitions. Each partition corresponds to one preamble sequence s_m^l. Let $\mathbf{n}_m$ denote the set of consecutive values of n in the partition associated with preamble s_m^l. For example, $\mathbf{n}_1 = \{n^{\text{st}}, \ldots, n^{\text{end}}\}$, $0 \le n^{\text{st}}, n^{\text{end}} < N_{\text{IDFT}}$, denotes the set of values of n in the partition associated with the root sequence s_1^l. Then, $\mathbf{n}_2$ can be defined as $\{(n^{\text{end}}+1) \mod N_{\text{IDFT}}, \ldots, (n^{\text{end}} + \lfloor N_{\text{IDFT}}/M \rfloor) \mod N_{\text{IDFT}}\}$ and so on for all $m \in \mathcal{M}$. The maximum value of $c[n]$ in a given partition m, i.e., $\max_{n \in \mathbf{n}_m} c[n]$, is the correlation between the received signal and the corresponding preamble s_m^l. Hence, having an impulse at index n that exceeds a certain threshold indicates that the corresponding preamble was transmitted. The signature detection stage determines the set of estimated transmitted preambles $\mathbf{s}_e$ as follows:

$$\mathbf{s}_e = \{s_m^l \mid \max_{n \in \mathbf{n}_m} c[n] > C, \ m \in \mathcal{M}\}, \quad (7)$$

where C is a threshold value that is chosen to meet certain successful detection requirement. Note that we cannot employ channel equalization since the channel state information is not available at the base station as preamble transmission is the first communication between a device and the base station before any data transmission or channel estimation takes place.

In Fig. 4, a sample correlation function $c[n]$ is shown for the case of a single device sending an aggregated preamble with root index $l = 129$ to the base station. The receiver needs to detect both preamble sequences of one preamble pair per device transmission. In Fig. 4 (a), the received preambles can easily be identified in the absence of delay, channel noise, and fading. Hence, $\mathbf{s}_e = \{s_{53}^{129}, s_{39}^{129}\}$ since $c[n]$ has impulses at values of n that correspond to these two preambles. Fig. 4 (b) shows a case where AWGN and the extended typical urban (ETU) fading channel [13] may cause false alarms. When the detection threshold C is equal to 0.06, $\mathbf{s}_e = \{s_{53}^{129}, s_{39}^{129}\}$. When $C = 0.04$, we have $\mathbf{s}_e = \{s_{53}^{129}, s_{39}^{129}, s_a^{129}, s_b^{129}\}$, where s_a^{129} and s_b^{129} are detected although they were not transmitted by a device. This can be avoided by tuning the threshold C to meet certain detection or false alarm criteria.

In case of multiple transmitters, the preamble pair detection stage determines which preamble sequences belong to a single aggregated preamble. This stage creates a small subset of candidate preamble pairs which includes all possible pairs that can be formed by the preambles in $\mathbf{s}_e$. The set of estimated transmitted preamble pairs, denoted as $\mathbf{q}_e$, is determined by calculating the correlation between Y and the frequency domain representation of each candidate preamble pair $Q_{a,b}^l$. This correlation is denoted as $c_{a,b}$ and is given by

$$c_{a,b}[n] = \frac{1}{N_{\text{IDFT}}} \sum_{k=0}^{N_{\text{IDFT}}-1} Y[k](Q_{a,b}^l[k])^* \exp\left(\frac{j2\pi kn}{N_{\text{IDFT}}}\right), \quad 0 \le n < N_{\text{IDFT}}. \tag{8}$$

Note that the number of candidates is much smaller than the number of all preamble pairs. The preamble pairs that exceed a correlation threshold C', which is calculated based on the received signal power, are considered to be detected and are assigned to the following set:

$$\mathbf{q}_e = \{q_{a,b}^l \mid s_a^l, s_b^l \in \mathbf{s}_e, c_{a,b}[n] > C'\}. \tag{9}$$

The proposed transmitter and receiver designs require only minor changes to the conventional PRACH transmitter and receiver. This makes the proposed preamble sequence design a preferable candidate to support mMTC.

IV. Performance Evaluation

In this section, we evaluate the PAPR, the probability of preamble collision, and the total service time of the proposed preamble sequence design, as well as the performance of the proposed receiver in terms of the probabilities of misdetection and false alarm. Throughout this section, equal power allocation is assumed where the two aggregated preambles are scaled equally, i.e., $\alpha_a = \alpha_b = \frac{1}{\sqrt{2}}$. This choice achieves an equal probability of detection at the receiver without prior knowledge of the selected preambles at the transmitter.

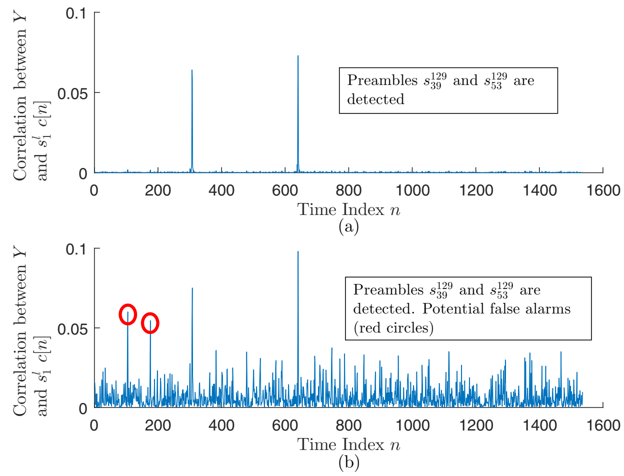

Fig. 4. Sample of correlation function $c[n]$. (a) In the absence of delay, noise, and channel fading, the transmitted preambles are detected successfully without any false alarms. (b) With AWGN and ETU fading channel, the receiver may detect false alarms (red circles).

A. PAPR Performance

We use the PAPR of the transmitted PRACH signals as a metric to evaluate the energy consumption of devices. Since most IoT devices are battery-powered, transmitting a signal with a high PAPR consumes more energy [14]. The PAPR of the transmitted signal $x[t]$, denoted as $\tau_{a,b}^{\alpha_a,\alpha_b}$, is defined as the ratio between its maximum power value and its average power, given that the preamble pair $q_{a,b}^l$ is selected and power scaling coefficients α_a and α_b are used.

$$\tau_{a,b}^{\alpha_a,\alpha_b} = (T_{\text{CP}} + T_{\text{SEQ}}) \times \frac{\max\{|x[0]|^2, \ldots, |x[T_{\text{CP}} + T_{\text{SEQ}} - 1]|^2\}}{\sum_{t=0}^{T_{\text{CP}}+T_{\text{SEQ}}-1} |x[t]|^2}, \tag{10}$$

where $T_{\text{CP}} + T_{\text{SEQ}}$ is the length of the transmitted signal $x[t]$.

Our goal is to form a set of preamble pairs for every given root index $l \in \mathcal{L}$, denoted as Λ^l, that includes the preamble pairs with PAPR less than a threshold $\tau_{\max} + \beta$. We define $\tau_{\max}$ as the maximum PAPR of all preambles s_m^l for all $m \in \mathcal{M}$ and $l \in \mathcal{L}$. β is the tolerance threshold. Λ^l can be expressed as

$$\Lambda^l = \{q_{a,b}^l \mid 10\log_{10}(\tau_{a,b}^{\alpha_a,\alpha_b}) \le \tau_{\max} + \beta\}, \quad \forall\, l \in \mathcal{L}. \tag{11}$$

When β is equal to 0 dB, we select only the preamble pairs whose PAPR does not exceed the maximum PAPR of conventional LTE preambles. Hence, the number of random access preambles available with our proposed sequence design is reduced, which results in a higher probability of preamble collision. On the other hand, setting $\beta > 0$ dB enables Λ^l to include preamble pairs whose PAPR is less than $\tau_{\max} + \beta$, which leads to having more preamble pairs in Λ^l compared to the case of $\beta = 0$ dB. Hence, β can be used to balance the PAPR and the probability of preamble collision. When β is set to ∞ dB, all the 2,016 preamble pairs are considered without any PAPR constraint.

In Fig. 5, we show the cumulative distribution function of the PAPR of all the preambles at all $N_{zc} - 1$ root sequences

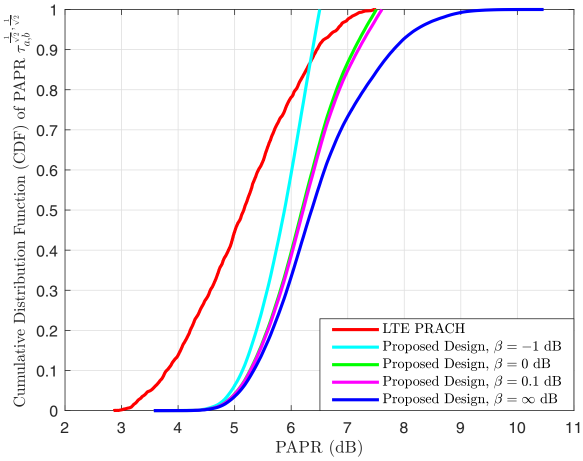

Fig. 5. The CDF of the PAPR for different values of tolerance threshold β. As β decreases, we select preamble pairs with lower PAPRs which enhances the PAPR performance but reduces the number of available preamble pairs.

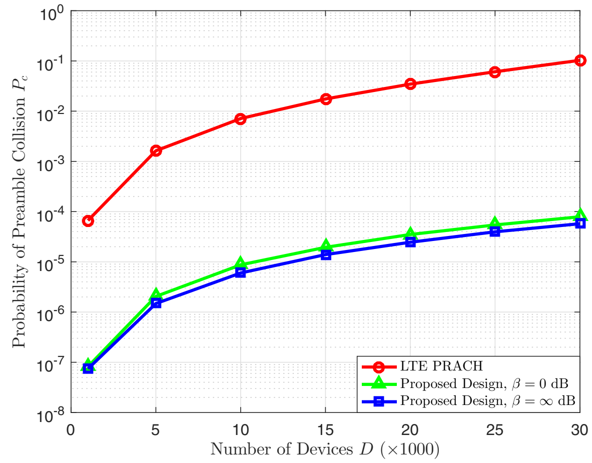

Fig. 6. The probability of preamble collision versus D for different preamble sequence designs with uniform arrival process and retransmissions.

for preamble format 0 [5], i.e., $N_{zc} = 839$. We set τ_{max} to be 7.5 dB and vary the PAPR tolerance threshold β which affects the number of preambles pairs that satisfy the PARR threshold criterion. As β decreases, Λ^l has fewer preamble pairs that can be used but the maximum and median PAPR decrease which reduces the energy consumption. The average number of available preambles per root is equal to $\frac{1}{N_{zc}-1}\sum_{l\in\mathcal{L}} \mathbf{card}(\Lambda^l)$, where $\mathbf{card}(\cdot)$ denotes the cardinality of a set. For example, if $\beta = 0$ and 0.1 dB, the average number of available preambles per root becomes $1{,}703$ and $1{,}742$ preamble pairs, respectively, rather than $2{,}016$ when $\beta = \infty$ dB.

B. Random Access Performance

We evaluate the random access performance using two metrics, which are the probability of preamble collision and the average total service time. The probability of preamble collision is the ratio between the number of preamble collision occurrences and the total number of preamble transmissions. It is a metric that indicates the capability of the proposed sequence design to support a larger number of devices due to increasing the number of preambles from 64 to $2{,}016$. We evaluate the probability of preamble collision in a simulation setup with the number of devices D varies from $1{,}000$ to $30{,}000$ devices that arrive according to a uniform arrival process over a period of 10 sec. Preamble retransmissions are allowed for up to 10 times. The backoff, RAR message, and contention window delays are taken into account with values of 20, 5, 48 ms, respectively [15]. Each device has a random access opportunity to start its random access procedure every 5 ms. The probability of preamble detection in case of no collision is equal to $(1 - 1/\exp(\text{transmission attempt index}))$ [15]. We consider the proposed sequence design when $\beta = 0$ dB (i.e., a subset of only $1{,}703$ preambles is considered to maintain a PAPR less that $\tau_{\text{max}} = 7.5$ dB) and $\beta = \infty$ dB (i.e., all $2{,}016$ preambles are considered). We compare the proposed design with conventional LTE PRACH (i.e., 64 preambles). Fig. 6 shows the simulation results of the probability of preamble collision. The results show that the proposed sequence design can be used to support mMTC with a probability of preamble collision of less than 10^{-4}. Furthermore, having a PAPR threshold to reduce energy consumption, which enables using fewer preambles per root, does not cause a significant increase in the collision probability. Hence, β can be adjusted to meet a certain preamble collision probability criterion.

The second metric is the average total service time. It is defined as the time taken until all the backlogged IoT devices successfully transmit a preamble without encountering a collision. At the first random access opportunity slot, there are between $1{,}000$ and $30{,}000$ devices that send randomly selected preambles. If a device encounters a preamble collision, it will backoff for a uniformly distributed random number of random access opportunity slots between 1 and 4. The slot corresponds to the period of time that includes one random access opportunity (e.g., 5 ms). We compare the performance between our proposed design with $\beta = 0$ dB and $\beta = \infty$ dB and the ACB scheme [6] in terms of the average total service time. In ACB, there are 64 preambles and the ACB probability of transmission is optimized, i.e. $p_{\text{ACB}} = \min\{1, \text{Number of preambles}/\text{Number of backlogged devices}\}$ [6]. It is assumed that the base station knows the total number of backlogged devices in the system. Fig. 7 shows the average total service time for different number of IoT devices. The results show that having a larger set of preambles outperforms using ACB since it can reduce the total service time by up to 83%. Note that, without ACB, having 64 preambles only may not be sufficient to serve devices within a finite delay constraint due to continuous preamble collisions.

C. Aggregated Preamble Detection Performance

We evaluate the proposed receiver design in terms of the probabilities of misdetection and false alarm. We consider the case where one IoT device randomly selects a preamble pair to transmit. All preamble pairs are chosen with equal probability. The preambles are transmitted over an ETU fading channel with a Doppler frequency of 70 Hz [13]. A uniform random delay is considered for the transmitted preamble signal. Preamble sequences are generated for preamble format

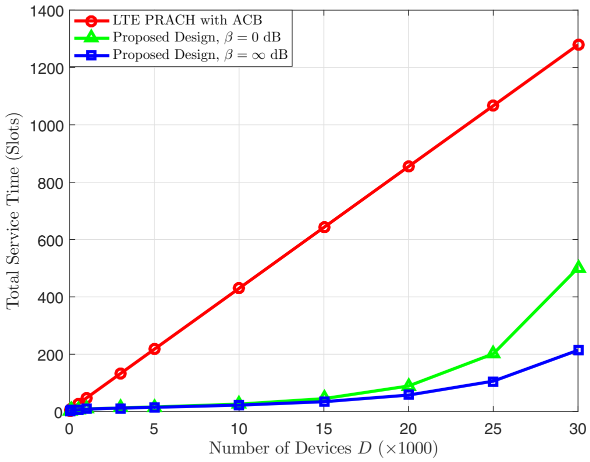

Fig. 7. The average total service time versus the number of devices D for different preamble sequence designs.

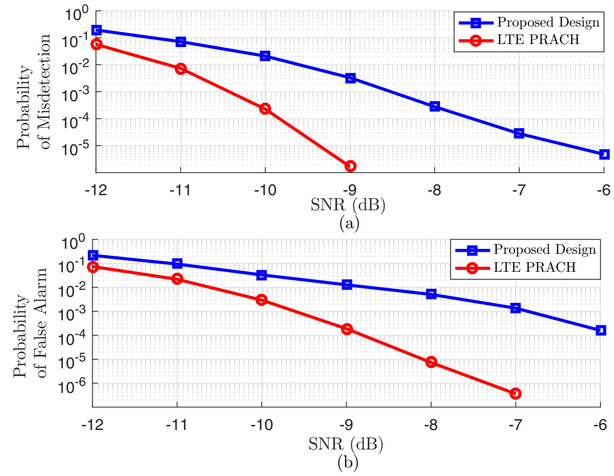

Fig. 8. (a) The probability of misdetection versus SNR. (b) The probability of false alarm versus SNR.

0 [5]. Hence, N_{zc} is equal to 839 and we select $N_{cs} = 13$, and thus we have $M = 64$ Zadoff-Chu preamble sequences. We vary the received SNR from -12 dB to -6 dB. We compare between the proposed receiver and the LTE PRACH receiver (with non-aggregated preamble transmission). We determine the average probabilities of misdetection and false alarm over all the 838 different roots.

The probability of misdetection is the ratio between the number of the transmitted preambles that are not detected and the total number of transmitted preambles. Results are shown in Fig. 8 (a). The detection of the aggregated preambles requires two preambles to be successfully detected while allocating each half of the transmit power. This causes the probability of misdetection of the proposed design to be higher than that of LTE PRACH. If the SNR exceeds -8 dB, then the probability of misdetection of the proposed receiver is less than 10^{-3}. In Fig. 8 (b), the probability of false alarm is shown. It is the ratio between the number of detected preambles that were not actually transmitted (e.g., incorrect detection decisions) and the total number of transmitted preambles. We note that the probability of false alarm of the proposed PRACH is maintained below 10^{-3} when the SNR exceeds -7 dB. The performance of the proposed receiver is better at higher SNR. In small cell deployments, the SNR is expected to be high due to low propagation loss. Hence, we can adopt this design for random access in small cell deployments supporting a massive number of IoT devices to make use of the improvement in the average total service time.

V. Conclusion

In this paper, we proposed a new preamble sequence design that is based on aggregating two Zadoff-Chu preamble sequences together to generate a larger set of random access preambles to support the mMTC use case. We proposed designs for both the transmitter and receiver that require minor changes compared to that of the conventional LTE PRACH designs. The proposed design reduces the probability of preamble collision to be less than 10^{-4}. Furthermore, we suggested selecting a subset of preambles that meet a certain PAPR threshold criterion to reduce energy consumption of battery-powered IoT devices. Simulation results showed that our proposed receiver can achieve low probabilities of misdetection and false alarm at sufficiently high SNR (e.g., SNR ≥ -7 dB). For future work, we will pair preamble sequences from different roots and study preamble sequence planning in multi-cell scenarios.

References

[1] Cisco, "Cisco visual networking index: Global mobile data traffic forecast update, 2016 - 2021," Feb. 2017.

[2] ITU-R M.2410-0, "Minimum requirements related to technical performance for IMT-2020 radio interface(s)," Nov. 2017.

[3] Next Generation Mobile Networks (NGMN) Alliance, "NGMN 5G white paper," Feb. 2015.

[4] A. Laya, L. Alonso, and J. Alonso-Zarate, "Is the random access channel of LTE and LTE-A suitable for M2M communications? A survey of alternatives," *IEEE Commun. Surveys & Tuts*, vol. 16, no. 1, pp. 4–16, First Quarter 2014.

[5] 3GPP TS 36.211 V15.2.0, "Physical channels and modulation (Release 15)," Jun. 2018.

[6] S. Duan, V. Shah-Mansouri, Z. Wang, and V. Wong, "D-ACB: Adaptive congestion control algorithm for bursty M2M traffic in LTE networks," *IEEE Trans. Veh. Technol.*, vol. 65, pp. 9847–9861, Dec 2016.

[7] K. Lee, J. Shin, Y. Cho, K. S. Ko, D. K. Sung, and H. Shin, "A group-based communication scheme based on the location information of MTC devices in cellular networks," in *Proc. of IEEE International Conference on Communications (ICC)*, Ottawa, Canada, Jun. 2012.

[8] Y. Liang, X. Li, J. Zhang, and Z. Ding, "Non-orthogonal random access (NORA) for 5G networks," *IEEE Trans. Wireless Commun.*, vol. 16, no. 7, pp. 4817–4831, Jul. 2017.

[9] R. Abbas, M. Shirvanimoghaddam, Y. Li, and B. Vucetic, "Random access for M2M communications with QoS guarantees," *IEEE Trans. Commun.*, vol. 65, no. 7, pp. 2889–2903, Jul. 2017.

[10] 3GPP:R1-1712357, "NR RACH preamble format for capacity enhancement," *3GPP TSG RAN WG1 Meeting 90, CATT*, Aug. 2017.

[11] 3GPP:R1-1711600, "PRACH preamble sequences and formats for capacity enhancement and beam management," *3GPP TSG RAN WG1 Adhoc Meeting, Huawei*, Jun. 2017.

[12] 3GPP TS 36.300 V15.2.0, "Overall description (Release 15)," Jun. 2018.

[13] 3GPP TS 36.104 V15.3.0, "Base station (BS) radio transmission and reception (Release 15)," Jun. 2018.

[14] S. H. Han and J. H. Lee, "An overview of peak-to-average power ratio reduction techniques for multicarrier transmission," *IEEE Wireless Commun.*, vol. 12, no. 2, pp. 56–65, Apr. 2005.

[15] 3GPP TR 37.868 V11.0.0, "Study on RAN improvements for machine-type communications," Sep. 2011.